Ferric microperoxidase-11 catalyzes peroxynitrite isomerization

Paolo Ascenzi [a,b,*], Loris Leboffe [a], Roberto Santucci [c], Massimo Coletta [c,d]

[a] Interdepartmental Laboratory for Electron Microscopy, Roma Tre University, I-00146 Roma, Italy
[b] Institute of Protein Biochemistry National Research Council, I-80131, Napoli, Italy
[c] Department of Clinical Sciences and Translational Medicine, University of Roma "Tor Vergata", I-00133 Roma, Italy
[d] Interuniversity Consortium for the Research on the Chemistry of Metals in Biological Systems, I-70126 Bari, Italy

ABSTRACT

Microperoxidase-11 (MP11) is an undecapeptide derived from horse heart cytochrome *c* offering the possibility to study the reactivity of the heme group relatively unshielded by the protein. Here, the peroxynitrite isomerization to NO_3^- catalyzed by ferric MP11 (MP11–Fe(III)) is reported. Data were obtained between pH 3.6 and 8.1, at 20.0 °C. The value of the second-order rate constant (k_{on}) for peroxynitrite isomerization to NO_3^- by MP11–Fe(III) decreases from $(1.1 \pm 0.1) \times 10^5\ M^{-1}\ s^{-1}$, at pH 3.6, to $(6.1 \pm 0.6) \times 10^3\ M^{-1}\ s^{-1}$, at pH 8.1. The pH dependence of k_{on} ($pK_a = 6.9$) suggests that peroxynitrous acid reacts preferentially with MP11–Fe(III). The MP11–Fe(III)-catalyzed isomerization of peroxynitrite to NO_3^- has been ascribed to the reactive penta-coordinated heme–Fe atom of MP11–Fe(III). In fact, cyanide binding to the sixth coordination position of the heme–Fe atom inhibits the MP11–Fe(III)-catalyzed isomerization of peroxynitrite to NO_3^-. The values of the first-order rate constant (k_0) for isomerization of peroxynitrite to NO_3^- in the presence of the MP11–Fe(III)–CN complex are superimposable to those obtained in the absence of MP–Fe(III). Values of k_{on} for peroxynitrite isomerization to NO_3^- by MP11–Fe(III) overlap those obtained for penta-coordinated cardiolipin–cytochrome *c* complex and for carboxymethylated cytochrome *c* in absence and presence of cardiolipin. Present results highlight the role of the heme–Fe(III) co-ordination state in the modulation of cytochrome *c* reactivity.

© 2014 Elsevier Inc. All rights reserved.

1. Introduction

Cytochrome *c* (cyt *c*) fulfills electron transfer roles in several vital processes of living organisms, including respiration, photosynthesis, and fermentation. The prosthetic group of cyt *c* is formed from the condensation of heme *b* with two protein Cys residues. The fifth coordination ligand of the heme–Fe atom of cyt *c* (*i.e.*, the proximal endogenous ligand) is invariantly His, whereas the sixth endogenous coordination ligand exhibits high variability, being Met in horse heart cyt *c* [1–5].

The heme–Fe atom of hexa-coordinated native horse heart cyt *c* is essentially unreactive whereas the heme–Fe atom of penta-coordinated carboxymethylated cyt *c* (CM-cyt *c*), cardiolipin-bound CM-cyt (CL-CM-cyt *c*), and cardiolipin-bound cyt *c* (CL-cyt *c*) is able to bind exogenous ligands. The reactivity of penta-coordinated ferrous and/or ferric CM-cyt *c*, CL-CM-cyt *c*, and CL-cyt *c* has been deeply investigated, highlighting the modulating role of the distal Met80–Fe bond. In particular, the redox properties, as well as the kinetic and/or thermodynamic

parameters for heme-Fe-based reactions, including carbonylation, nitrosylation, reductive nitrosylation, peroxynitrite isomerization to NO_3^-, nitrite reduction to NO, and peroxidation, have been reported [6–20].

Microperoxidase-11 (MP11) is an excellent model compound, useful to dissect the modulatory role of the protein matrix from the intrinsic catalytic properties of penta-coordinated heme *c*. In fact, MP11 is a heme–peptide complex formed by eleven amino acid residues and a heme *c* covalently-linked to the proximal site by the Cys-Xxx-Xxx-Cys-His sequence, which is highly conserved within most cyt *c* (Fig. 1) [1–5,21]. Unlike most members of the cyt *c* family, which are hexa-coordinated in both ferrous and ferric states [1–5], MP11 is penta-coordinated, the sixth heme–Fe coordination ligand being the O atom of a water molecule in the ferric form (Fig. 1) [21]. Moreover, MP11 is a model compound of choice to study the effects of axial ligation on the spectroscopic and functional properties of cyt *c* [21].

Here, kinetics of MP11–Fe(III)-catalyzed isomerization of peroxynitrite to NO_3^- is reported. Peroxynitrite isomerization is catalyzed by penta-coordinated MP11–Fe(III) while hexa-coordinated MP11–Fe(III)–CN is non-reactive, this clearly demonstrates that the efficiency of catalysis reflects the heme–Fe(III) accessibility. Moreover, the HOONO species preferentially reacts with MP11–Fe(III). Values of k_{on} for peroxynitrite isomerization by penta-coordinated MP11–Fe(III) overlap those obtained for penta-coordinated CL-cyt *c*, CM-cyt *c*, and CL-CM-cyt *c*.

* Corresponding author at: Interdepartmental Laboratory for Electron Microscopy, Roma Tre University, Via della Vasca Navale 79, I-00146 Roma, Italy. Tel.: +39 06 5733 3621; fax: +39 06 5733 6321.
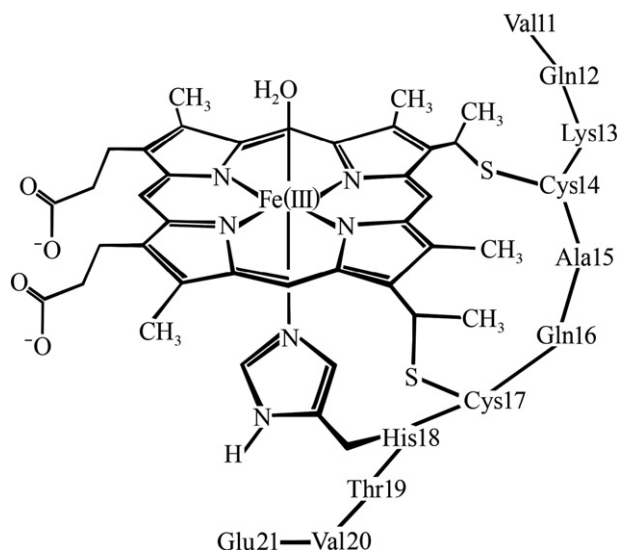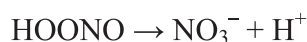*E-mail address:* ascenzi@uniroma3.it (P. Ascenzi).

Fig. 1. The MP11–Fe(III) structure. The numbering of the amino acid residues corresponds to that of horse heart cyt *c*.

$$k_0$$

$$\text{HOONO} \rightarrow \text{NO}_3^- + \text{H}^+$$

Scheme 1. Reaction mechanism for spontaneous peroxynitrite isomerization.

2. Materials

MP11–Fe(III) was obtained from Sigma-Aldrich (St. Louis, MO, USA). The MP11–Fe(III) concentration was determined spectrophotometrically at 395 nm ($\varepsilon = 1.23 \times 10^5$ M^{-1} cm^{-1} at pH 7.2 and 20.0 °C) [22]. The MP11–Fe(III) solution was prepared by dissolving the undecapeptide–heme–Fe(III) adduct in the 1.0×10^{-1} M sodium phosphate buffer, pH values ranged between pH 3.6 and 8.1. The final MP11–Fe(III) concentration ranged between 1.0×10^{-6} M and 5.0×10^{-5} M.

Peroxynitrite was purchased from Caiman Chemical Company (Ann Arbor, MI, USA). Nitrate and nitrite contaminations were less than 10%. The term peroxynitrite refers generically to both ONOO$^-$ and its conjugate acid HOONO [23–25]. Peroxynitrite was diluted immediately before use with degassed 1.0×10^{-2} M NaOH to reach the desired concentration. The final peroxynitrite concentration ranged between 2.5×10^{-5} M and 1.0×10^{-3} M [25–29]. The concentration of peroxynitrite was determined spectrophotometrically prior to each experiment by measuring the absorbance at 302 nm ($\varepsilon_{302\ nm} = 1.705 \times 10^3$ M^{-1} cm^{-1}) [30,31].

Experiments in the presence of cyanide at pH 7.2 (1.0×10^{-1} M sodium phosphate buffer) were carried out by adding 5.0×10^{-4} M cyanide to the MP11–Fe(III) and peroxynitrite solutions. This cyanide concentration allowed to obtain more than 90% of MP11–Fe(III)-cyanide complex (MP11–Fe(III)–CN) [22].

All the other chemicals were obtained from Merck AG (Darmstadt, Germany). All products were of analytical or reagent grade and were used without further purification.

3. Methods

3.1. Kinetics of peroxynitrite isomerization by MP11–Fe(III)

Kinetics of peroxynitrite isomerization by MP11–Fe(III), MP11–Fe(III)–CN (final concentration, 1.0×10^{-6} M to 1.2×10^{-5} M), and phosphate buffer (1.0×10^{-1} M) solutions was monitored at 302 nm, the characteristic absorbance maximum of peroxynitrite [30,31]. The peroxynitrite concentration ranged between 2.5×10^{-5} M and 1.0×10^{-3} M.

Kinetic data were obtained by rapid mixing the MP11–Fe(III), MP11–Fe(III)–CN, and phosphate buffer solutions with peroxynitrite solution using the SMF-400 rapid-mixing stopped-flow apparatus (Bio-Logic SAS, Claix, France). The light path of the observation cuvette was 10 mm and the dead-time was 1.4 ms.

Kinetics was obtained at 20.0 °C and between pH 3.6 and 8.1 (1.0×10^{-1} M phosphate buffer); the pH was always measured at the end of the reaction. No gaseous phase was present.

Between pH 3.6 and 8.1 and under conditions where the MP11–Fe(III) and MP11–Fe(III)–CN concentration ranged between 1.0×10^{-6} M and 1.2×10^{-5} M and the peroxynitrite concentration was 1.0×10^{-4} M, kinetics of peroxynitrite isomerization in the absence and presence of MP11–Fe(III) and MP11–Fe(III)–CN were analyzed in the framework of the minimum reaction Schemes 1 and 2, respectively [24,25]:

Values of the first-order rate constant for peroxynitrite isomerization in the presence of MP11–Fe(III)–CN, and 1.0×10^{-1} M phosphate buffer (*i.e.*, k_0), and of the pseudo-first-order rate constant for MP11–Fe(III)-mediated peroxynitrite isomerization (*i.e.*, k_{obs}) have been determined between pH 3.6 and 8.1, at 20.0 °C, from the analysis of the time-dependent absorbance decrease at 302 nm, according to Eq. (1) [23–25,29,32,33]:

$$[\text{peroxynitrite}]_t = [\text{peroxynitrite}]_i \times e^{-k \times t} \qquad (1)$$

where k is k_0 or k_{obs}.

Values of the second-order rate constant for MP11–Fe(III)-mediated peroxynitrite isomerization (*i.e.*, k_{on}) and of k_0 have been determined between pH 3.6 and 8.1 at 20.0 °C, from the linear dependence of k_{obs} on the MP11–Fe(III) concentration according to Eq. (2) [24,25,32]:

$$k_{obs} = k_{on} \times [\text{MP11-Fe(III)}] + k_0 \qquad (2)$$

At pH 3.6 and under conditions where the MP11–Fe(III) concentration was 5.0×10^{-6} M and the peroxynitrite concentration ranged from 2.5×10^{-5} M to 1.0×10^{-3} M, kinetics of peroxynitrite isomerization in the presence of MP11–Fe(III) were analyzed in the framework of the minimum reaction Schemes 1 and 3 [24,25]:
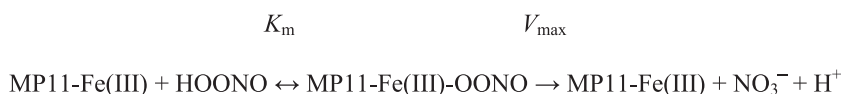
Values of the apparent dissociation equilibrium constant for peroxynitrite binding to MP11–Fe(III) (*i.e.*, K_m), of the apparent maximum velocity (*i.e.*, V_{max}), and of k_0 have been determined from the dependence of k_{obs} on the peroxynitrite concentration according to Eq. (3):

$$k_{obs} = ((V_{max} \times [\text{peroxynitrite}])/(K_m + [\text{peroxynitrite}])) + k_0 \qquad (3)$$

$$k_{on} \qquad\qquad\qquad fast$$

$$\text{MP11-Fe(III)} + \text{HOONO} \rightarrow \text{MP11-Fe(III)-OONO} \rightarrow \text{MP11-Fe(III)} + \text{NO}_3^- + \text{H}^+$$

Scheme 2. Reaction mechanism for peroxynitrite isomerization by MP11–Fe(III).

$$K_m \qquad\qquad\qquad V_{max}$$

$$MP11\text{-}Fe(III) + HOONO \leftrightarrow MP11\text{-}Fe(III)\text{-}OONO \rightarrow MP11\text{-}Fe(III) + NO_3^- + H^+$$

Scheme 3. Enzymatic mechanism for peroxynitrite isomerization by MP11−Fe(III).

The value of the apparent second-order rate constant for the formation of the MP11–Fe(III)–OONO complex (*i.e.*, k_{on} ($= V_{max} / K_m$)) has been also determined from the dependence of k_{obs} on the peroxynitrite concentration according to Eq. (4):

$$k_{obs} = k_{on} \times [peroxynitrite] + k_0 \tag{4}$$

under conditions where [peroxynitrite] $\ll K_m$. Of note, Eq. (3) reduces to Eq. (4) under conditions where [peroxynitrite] $\ll K_m$.

The pH-dependence of k_0 and k_{on} for peroxynitrite isomerization in the absence and presence of MP11–Fe(III) allowed to obtain, at 20.0 °C, values of pK_a and $k_{lim(top)}$ according to Eq. (5) [23–25]:

$$k = \left(\left(k_{lim(top)} \times 10^{-pH} \right) / \left(10^{-pH} + 10^{-pKa} \right) \right) \tag{5}$$

where k is k_0 or k_{on}, and $k_{lim(top)}$ represents the top asymptotic value of k under conditions where pH $<<$ pK_a.

3.2. NO_2^- and NO_3^- determination

NO_2^- and NO_3^- analysis was carried out spectrophotometrically at 543 nm by using the Griess reagent and VCl_3 to catalyze the conversion of NO_3^- to NO_2^-, as described previously [24,34,35]. Calibration curves were obtained by measuring 4-8 standard sodium nitrite and sodium nitrate solutions in 1.0×10^{-1} M phosphate buffer, pH 7.2 and 20.0 °C. The samples were prepared by mixing 500 μL of a MP11–Fe(III) solution (final concentration, 5.0×10^{-5} M in 1.0×10^{-1} M phosphate buffer, pH 7.2) with 500 μL of a peroxynitrite solution (final concentration, 2.0×10^{-4} M in 1.0×10^{-2} M NaOH), at 20.0 °C, in the absence and presence of cyanide ($= 5.0 \times 10^{-4}$ M). The reaction mixture was analyzed within *ca.* 10 min.

3.3. Data analysis

Kinetic and thermodynamic data were analyzed using the MatLab program (The Math Works Inc., Natick, MA, USA). The results are given as mean values of at least four experiments plus or minus the corresponding standard deviation.

4. Results and discussion

Kinetics of peroxynitrite isomerization, in the absence and presence of MP11–Fe(III) and MP11–Fe(III)–CN, was recorded by a single-wavelength stopped-flow apparatus. Under all the experimental conditions, a decrease of the absorbance at 302 nm was observed, as previously reported [36]. Kinetics of peroxynitrite isomerization was fitted to a single-exponential decay for more than $91 \pm 7\%$ of its course according to Eq. (1) (Fig. 2). According to literature [24,25], this indicates that no intermediate species (*e.g.*, MP11–Fe(III)–OONO; see Scheme 2) accumulate(s) in the course of peroxynitrite isomerization. In particular, the formation of the transient MP11–Fe(III)–OONO species represents the rate limiting step in catalysis, the conversion of MP11–Fe(III)–OONO to MP11–Fe(III) and NO_3^-/NO_2^- being faster by at
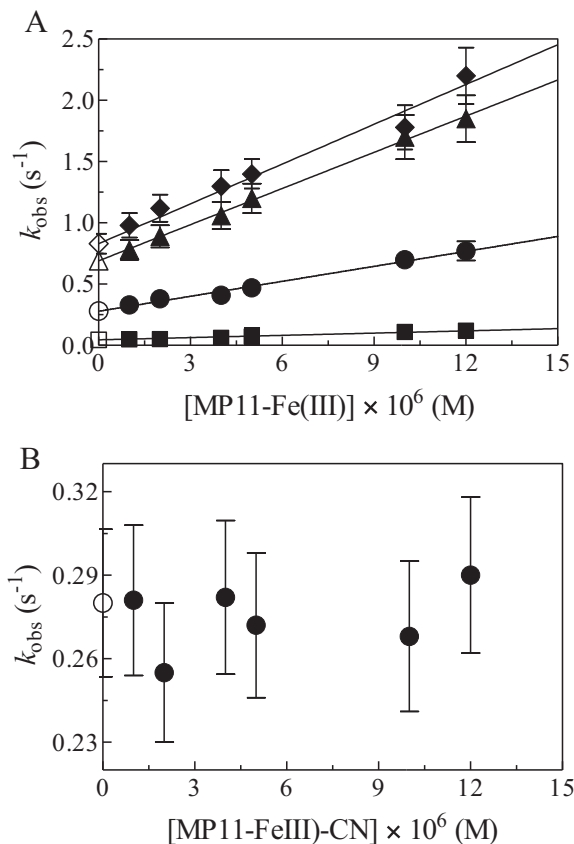
Fig. 3. Dependence of the pseudo-first-order rate constant for peroxynitrite isomerization (*i.e.*, k_{obs}) on the MP11–Fe(III) concentration (A), at pH 3.6 (filled diamonds), 6.2 (filled triangles), 7.2 (filled circles), and 8.1 (filled squares). The open symbols on the ordinate indicate values of k_0 obtained in the absence of MP11–Fe(III), at 3.6 (open diamonds), at pH 6.2 (open triangle), 7.2 (open circle), and 8.1 (open square). The continuous lines were calculated according to Eq. (2) with values of k_0 and k_{on} given in Table S1. Dependence of k_{obs} on the MP11–Fe(III)–CN concentration (B), at pH 7.2. The average k_{obs} value is 0.27 s^{-1}. The open circle on the ordinate indicates the k_0 value (0.28 s^{-1}) obtained in the absence of MP11–Fe(III) and MP11–Fe(III)–CN. The cyanide concentration was 5.0×10^{-4} M. The peroxynitrite concentration was 1.0×10^{-4} M. All data were obtained at 20.0 °C. Where not shown, standard deviation is smaller than the symbol. For details, see text.
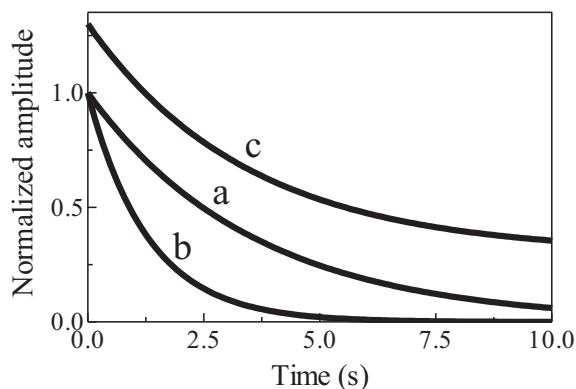

Fig. 2. Normalized averaged time courses of peroxynitrite isomerization in the absence (trace a) and presence of MP11–Fe(III) (trace b) and MP11–Fe(III)–CN (trace c), at pH 7.2. The analysis of data according to Eq. (1) allowed to determine the following values of $k_0 = 0.28$ s^{-1} (trace a), $k_{obs} = 0.77$ s^{-1} (trace b), and $k_{obs} = 0.29$ s^{-1} (trace c). For clarity, trace c has been offset by $+ 0.3$ units relative to traces a and b. The MP11–Fe(III) and MP11–Fe(III)–CN concentration was 1.2×10^{-5} M. The peroxynitrite concentration was 1.0×10^{-4} M. The cyanide concentration was 5.0×10^{-4} M. All data were obtained at 20.0 °C. For details, see text.

least one order of magnitude than the MP11–Fe(III)–OONO complex formation.

Over the whole pH range explored (from 3.6 to 8.1), the observed rate constant for MP11–Fe(III)-catalyzed isomerization of peroxynitrite (*i.e.*, k_{obs}) increases linearly with the MP11–Fe(III) concentration (Fig. 3, panel A). The analysis of data reported in Fig. 3 (panel A), according to Eq. (2), allowed the determination of values of the second-order rate constant for peroxynitrite isomerization by MP11–Fe(III) (k_{on}; corresponding to the slope of the linear plots) and of the first-order rate constant for peroxynitrite isomerization in the absence of MP11–Fe(III) (k_0; corresponding to the *y* intercept of the linear plots). Values of k_{on} and k_0 obtained between pH 3.6 and 8.1 are reported in Table S1. Values of k_0 for peroxynitrite isomerization in the absence of MP11–Fe(III) (Table S1) are in good agreement with those obtained in the absence and presence of MP11–Fe(III)–CN (Fig. 3, panel B) and those reported in the literature [23–25,33]. This indicates that the acceleration of the peroxynitrite isomerization rate by MP11–Fe(III) (*i.e.*, k_{obs} *versus* k_0) is due to the reaction of peroxynitrite with the heme–Fe(III) atom, which is inhibited by cyanide. This result agrees with previous observations concerning the isomerization kinetics of peroxynitrite by cyanide-bound ferric horse heart myoglobin (Mb), human hemoglobin (Hb), and human serum heme–albumin (SA–heme–Fe) [24,37].

To confirm the catalytic effect of MP11–Fe(III) on peroxynitrite isomerization, the dependence of k_0 and k_{obs} on the peroxynitrite concentration was determined in the absence and presence of MP11–Fe(III) and MP11–Fe(III)–CN concentration, at pH 3.6 and 7.2 (Figs. 4 and 5).

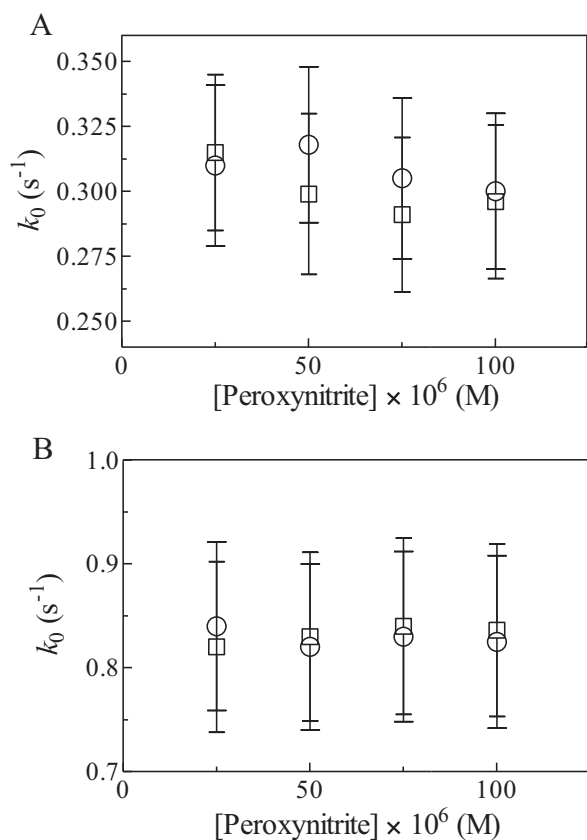Under all the experimental conditions, the amplitude of kinetics for peroxynitrite isomerization increases as a function of the peroxynitrite concentration (data not shown). At pH 7.2, values of k_0 and k_{obs} slightly decrease on increasing the peroxynitrite concentration (Figs. 4, panel A, and 5, panel A). This behavior has been postulated to reflect the occurrence of the ONOO⁻/HOONO dimeric adduct at high peroxynitrite concentration (>5.0 × 10⁻⁵ M), around neutrality [24]. Accordingly, the decrease of k_0 and k_{obs} values on increasing the peroxynitrite concentration may reflect either the slow MP11–Fe(III)-mediated decomposition of the ONOO⁻/HOONO dimeric adduct or the slow dissociation of the ONOO⁻/ONOOH dimeric adduct preceding MP11–Fe(III)-catalyzed isomerization of peroxynitrite [24]. In contrast, values of k_0 are independent of the peroxynitrite concentration (Fig. 4, panel B), and values of k_{obs} increase with the peroxynitrite concentration (Fig. 5, panel B), at pH 3.6. This may reflect the occurrence of the very low level of ONOO⁻ at pH 3.6 (~0.1%; the pK_a value of ONOO⁻/ONOOH being ~6.8 [33,37,38]), which impairs the formation of the ONOO⁻/HOONO dimeric adduct. At pH 3.6, the analysis of the dependence of k_{obs} on the peroxynitrite concentration according to Eq. (3) allowed to estimate the apparent dissociation equilibrium constant for peroxynitrite binding to MP11–Fe(III) ($K_m = (6.7 \pm 0.7) \times 10^{-4}$ M) and of the maximum velocity for peroxynitrite isomerization ($V_{max} = 74.4 \pm 0.7$ s⁻¹). Moreover, as expected for a simple reaction, the value of k_{on} obtained at pH 3.6 under conditions where the MP11–Fe(III) concentration ranges from 1.0×10^{-6} M to 1.2×10^{-5} M and the peroxynitrite concentration is 1.0×10^{-4} M (according to Eq. (2)) corresponds to that determined under conditions where the MP11–Fe(III) concentration is 5.0×10^{-6} M and the peroxynitrite concentration ranges from

Fig. 4. Effect of peroxynitrite concentration on values of the first-order rate constant for peroxynitrite isomerization in the presence of MP11–Fe(III)–CN (*i.e.*, k_0; open squares) and 1.0×10^{-1} M phosphate buffer (*i.e.*, k_0; open circles), at pH 7.2 (A) and 3.6 (B) and 20.0 °C. The cyanide concentration was 5.0×10^{-4} M. The MP11–Fe(III)–CN concentration was 5.0×10^{-6} M. For details, see text.
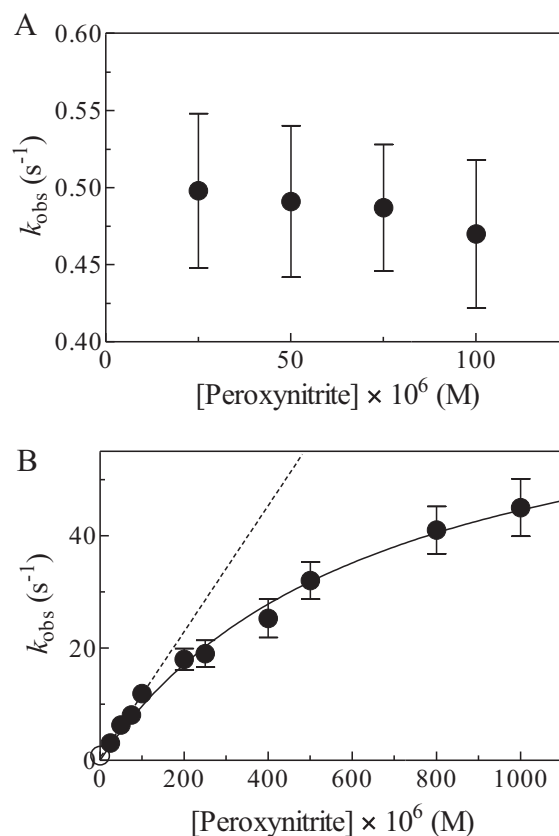

Fig. 5. Effect of peroxynitrite concentration on values of the pseudo-first-order rate constant for peroxynitrite isomerization in the presence of MP11–Fe(III) (*i.e.*, k_{obs}), at pH 7.2 (A) and 3.6 (B) and 20.0 °C. the MP11–Fe(III) concentration was 5.0×10^{-6} M. In panel B, the open circle on the ordinate indicates the value of k_0 obtained in the absence of MP11–Fe(III). The continuous line in panel B was calculated according to Eq. (3), with $K_m = (6.7 \pm 0.7) \times 10^{-4}$ M, $V_{max} = 74.4 \pm 0.7$ s⁻¹, and $k_0 = 0.83 \pm 0.08$ s⁻¹; the value of k_{on} (= V_{max} / K_m) is 1.1×10^5 M⁻¹ s⁻¹. The dashed line in panel B was calculated according to Eq. (4), with values of k_0 and k_{on} given in Table S1. The MP11–Fe(III) concentration was 5.0×10^{-6} M. For details, see text.
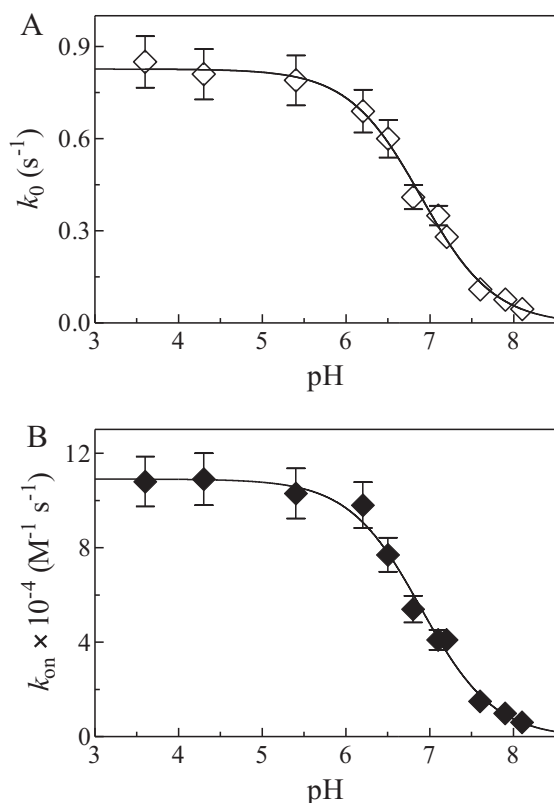
Fig. 6. Effect of pH on the first-order rate constant for peroxynitrite isomerization (*i.e.*, k_0; A). Values of k_0 are the average of those obtained in the absence and presence of MP11–Fe(III) (see Table S1). The continuous line was calculated according to Eq. (4) with $pK_a = 6.9 \pm 0.2$ and $k_{lim(top)} = 0.83 \pm 0.09 \, s^{-1}$. Effect of pH on the second-order rate constant for MP11–Fe(III)-mediated peroxynitrite isomerization (*i.e.*, k_{on}; B). The continuous line was calculated according to Eq. (5) with $pK_a = 6.9 \pm 0.2$ and $k_{lim(top)} = (1.1 \pm 0.1) \times 10^5 \, M^{-1} \, s^{-1}$. The peroxynitrite concentration was 1.0×10^{-4} M. All data were obtained at 20.0 °C. Where not shown, standard deviation is smaller than the symbol. For details, see text.

2.5×10^{-5} M to 1.0×10^{-3} M (according to Eq. (4)) (Figs. 3, panel A, 5, panel B, and Table S1).

The pH dependence of k_0 and k_{on} for peroxynitrite isomerization, in the absence and presence of MP11–Fe(III), was examined to identify tentatively the species that preferentially react(s) with MP11–Fe(III). Values of k_0 and k_{on} for peroxynitrite isomerization in the absence and presence of MP11–Fe(III), respectively, decrease on increasing pH from 3.6 to 8.1 (Fig. 6). The analysis of data reported in Fig. 6, according to Eq. (5), indicates that values of pK_a for the pH dependence of k_0 ($pK_a = 6.9 \pm 0.2$) (Fig. 6, panel A) and of k_{on} ($pK_a = 6.9 \pm 0.2$) (Fig. 6, panel B) are essentially the same within the error limit. The pK_a values for the pH dependence of k_0 and k_{on} here determined are in excellent agreement with pK_a values reported in the literature [24, 25,33,37,38]. Accordingly, the close similarity of the pH dependence of k_0 (Fig. 6, panel A) and of k_{on} (Fig. 6, panel B) suggests that under all

Table 1
NO_3^- and NO_2^- distribution of peroxynitrite isomerization in the absence and presence of MP11–Fe(III), and MP11–Fe(III)–CN, at pH 7.2 and 20.0 °C. [a]

MP11–Fe(III) (M)	MP11–Fe(III)–CN [b] (M)	$[NO_3^-]$ (%)	$[NO_2^-]$ (%)	$[NO_3^-] + [NO_2^-]$ (%)
–	–	81 ± 6	17 ± 4	98 ± 10
1.0×10^{-5}	–	91 ± 6	8 ± 3	99 ± 9
–	1.0×10^{-5}	79 ± 5	22 ± 3	101 ± 8

[a] The MP11–Fe(III) concentration was 5.0×10^{-5} M, and the peroxynitrite concentration was 2.0×10^{-4} M.
[b] The cyanide concentration was 5.0×10^{-4} M.

Table 2
Peroxynitrite scavenging by ferric heme–proteins and heme-model compounds.

Heme protein or heme-model compound	k_{on} ($M^{-1} \, s^{-1}$)
Methanosarcina acetivorans Pgb Cys101(E20)Ser mutant [a]	3.8×10^4
Mycobacterium tuberculosis truncated-Hb N [b]	6.2×10^4
Pseudoalteromonas haloplanktis TAC125 truncated-Hb O [c]	2.9×10^4
Horse heart Mb [d]	2.9×10^4
Sperm whale Mb [e]	1.6×10^4
Sperm whale Mb His64(E7)Ala mutant [e]	5.8×10^6
Sperm whale Mb His64(E7)Asp mutant [e]	4.8×10^6
Sperm whale Mb His64(E7)Leu mutant [e]	5.7×10^4
Sperm whale Mb Phe43(CD1)Trp/His64(E7)Leu mutant [e]	5.2×10^4
Sperm whale Mb His64(E7)Tyr/His97(F8)Gly mutant [e]	9.0×10^3
Human Hb [f]	1.2×10^4
Human SA–heme [g]	4.1×10^5
Ibuprofen–human SA–heme [h]	3.5×10^4
Truncated human SA–heme [i]	4.3×10^5
Ibuprofen–truncated human SA–heme [j]	5.8×10^4
CL-cyt *c* [k]	3.2×10^5
CM-cyt *c* [l]	6.8×10^4
CL-CM-cyt *c* [l]	5.3×10^5
Fusarium oxysporum cytochrome P450 NO reductase [m]	$\sim5 \times 10^5$
FeTMPS [n]	6.0×10^4
MP11 [o]	4.1×10^4

[a] pH = 7.4 and 20.0 °C. From [44].
[b] pH 7.0 and 20.0 °C. From [42].
[c] pH 7.0 and 20.0 °C. From [43].
[d] pH 7.0 and 20.0 °C. From [24].
[e] pH 7.5 and 20.0 °C. From [25].
[f] pH 7.5 and 20.0 °C. From [24].
[g] pH 7.2 and 22.0 °C. From [37].
[h] pH 7.2 and 22.0 °C. Ibuprofen was 1.0×10^{-2} M. From [37].
[i] pH 7.0 and 20.0 °C. From [41].
[j] pH 7.0 and 20.0 °C. Ibuprofen was 1.0×10^{-2} M. From [41].
[k] pH 7.0 and 20.0 °C. CL was 1.6×10^{-4} M. From [12].
[l] pH 7.0 and 20.0 °C. CL was 1.6×10^{-4} M. From [13].
[m] pH 8.0 and 12.0 °C. From [39].
[n] pH 7.6 and 25.0 °C. From [40].
[o] pH 7.2 and 20.0 °C. Present study.

experimental conditions HOONO is the species that preferentially undergoes isomerization.

As shown in Table 1, the spontaneous isomerization of peroxynitrite yielded $80 \pm 6\%$ NO_3^- and $20 \pm 4\%$ NO_2^-, and (the NO_3^- and NO_2^- yields increased ($91 \pm 5\%$) and decreased ($8 \pm 3\%$), respectively, in the presence of MP11–Fe(III). These results agree with those previously obtained for the spontaneous isomerization of peroxynitrite and for the ferric horse heart Mb-, human Hb-, and human SA–heme-catalyzed isomerization of peroxynitrite [24,37].

Peroxynitrite isomerization is catalyzed by penta-coordinated MP11–Fe(III), while hexa-coordinated MP11–Fe(III)–CN is non-reactive (Figs. 3 and 4). This demonstrates that the efficiency of the catalytic process reflects the access to and the coordination of the heme–Fe(III) atom. The values of k_{on} for peroxynitrite isomerization by ferric heme–proteins and heme-model compounds range between $9.0 \times 10^3 \, M^{-1} \, s^{-1}$ and $5.8 \times 10^6 \, M^{-1} \, s^{-1}$ (Table 2) (see [12,13,24,25,37,39–44] and present study), reflecting the coordination of the heme–Fe(III) atom. In fact, cardiolipin (CL) binding facilitates peroxynitrite isomerization by wild-type and carboxymethylated ferric horse heart cyt *c* inducing the cleavage or the severe weakening of the sixth coordination bond of the heme–Fe(III) atom [12,13,45]. In contrast, ibuprofen binding to the FA2 site of ferric wild-type and truncated human SA-heme induces the hexa-coordination of the heme–Fe(III) atom, with the consequent inhibition of the heme-based reactivity [37,41,46]. Also, hexa-coordinated ferric horse heart cyt *c* and human neuroglobin [47,48] do not catalyze the peroxynitrite conversion to NO_3^- [12,49]. Moreover, the analysis of k_{on} values for peroxynitrite isomerization by wild-type and mutants of sperm whale Mb(III) (see Table 2) suggests that the heme–Fe(III) reactivity is regulated not only by steric factors modulating the ligand access to the metal center, but also by the Lewis acidity of the heme–Fe(III)

atom [25]. In fact, the His64(E7)Ala and His64(E7)Asp mutations facilitate the ligand access to the heme–Fe(III) center and the peroxynitrite isomerization to NO_3^- [25]. In contrast, the low reactivity of His64(E7) Leu and Phe43(CD1)Trp/His64(E7)Leu mutants has been attributed to the steric hindrance of the Leu64(E7) residue, which limits the peroxynitrite access to the heme–Fe(III) center [25]. Furthermore, the low k_{on} value of the His64(E7)Tyr/His97(F8)Gly mutant has been ascribed to either a limited accessibility of peroxynitrite to the catalytic center or the reduced Lewis acidity of the heme–Fe(III) atom, as a consequence of the Tyr64(E7) residue binding [25].

In conclusion, it is interesting to point out that, in spite of the sterically open access for the exogenous ligand, the reactivity of MP11–Fe(III) with peroxynitrite falls in a slower range of values for k_{on} (even two orders of magnitude lower, see Table 2) with respect to the sperm whale Mb mutants having a penta-coordinated heme–Fe(III) atom (thus, not a high-spin hexa-coordinated H_2O-bound heme–Fe(III) atom, as in MP11–Fe(III) and in wild type sperm whale Mb). This strengthens the hypothesis that, in addition to the steric hindrance of the protein moiety, peroxynitrite reactivity is critically modulated by the heme–Fe(III) atom coordination and Lewis acidity.

5. Conclusion

Heme-model compounds may play a primary role for dissecting the distinct contributions leading to the physico-chemical properties shown by a heme–protein. In particular, the roles played by the protein moiety and the metal active site may be better differentiated through this kind of approach. Moreover, heme-model compounds may provide an important contribution for the construction of chimeric proteins with novel active sites, potentiating and/or diversifying the enzymatic activity of a protein [21,50,51]. In this respect, complexes of human SA with hemes, phthalocyanines, and microperoxidases display metal-based catalysis and have been postulated to play a relevant role(s) in biotechnological applications [52].

Abbreviations

CL	cardiolipin
CL-cyt *c*	CL-bound cyt *c*
CM-cyt *c*	carboxymethylated-cyt *c*
cyt *c*	cytochrome *c*
FeTMPS	iron(III) *meso*-tetra(2,4,6-trimethyl-3,5-disulfonato)porphine chloride
Hb	hemoglobin
Mb	myoglobin
MP11	microperoxidase containing 11 amino acid residues
MP11–Fe(III)	ferric MP11
Pgb	protoglobin
SA	serum albumin
SA-heme	serum heme–albumin

Appendix A. Supplementary data

Supplementary data to this article can be found online at http://dx.doi.org/10.1016/j.jinorgbio.2014.12.013.

References

[1] I. Bertini, G. Cavallaro, A. Rosato, Chem. Rev. 106 (2006) 90–115.
[2] Y.P. Ow, D.R. Green, Z. Hao, T.W. Mak, Nat. Rev. Mol. Cell Biol. 9 (2008) 532–542.
[3] J.M. Stevens, Metallomics 3 (2011) 319–322.
[4] D.A. Mavridou, S.J. Ferguson, J.M. Stevens, IUBMB Life 65 (2013) 209–216.
[5] S. Zaidi, M.I. Hassan, A. Islam, F. Ahmad, Cell. Mol. Life Sci. 71 (2014) 229–255.
[6] M.T. Wilson, M. Brunori, G.C. Rotilio, E. Antonini, J. Biol. Chem. 248 (1973) 8162–8169.
[7] M. Di Marino, R. Marassi, R. Santucci, M. Brunori, F. Ascoli, Bioelectrochem. Bioenerg. 17 (1987) 27–34.
[8] S. Oellerich, S. Lecomte, M. Paternostre, T. Heimburg, P. Hidebrandt, J. Phys. Chem. B 108 (2004) 3871–3878.
[9] L.V. Basova, I.V. Kurnikov, L. Wang, V.B. Ritov, N.A. Belikova, I.I. Vlasova, A.A. Pacheco, D.E. Winnica, J. Peterson, H. Bayir, D.H. Waldeck, V.E. Kagan, Biochemistry 46 (2007) 3423–3434.
[10] S.M. Kapetanaki, G. Silkstone, I. Husu, U. Liebl, M.T. Wilson, M.H. Vos, Biochemistry 48 (2009) 1613–1619.
[11] G. Silkstone, S.M. Kapetanaki, I. Husu, M.H. Vos, M.T. Wilson, J. Biol. Chem. 285 (2010) 19785–19792.
[12] P. Ascenzi, C. Ciaccio, F. Sinibaldi, R. Santucci, M. Coletta, Biochem. Biophys. Res. Commun. 404 (2011) 190–194.
[13] P. Ascenzi, C. Ciaccio, F. Sinibaldi, R. Santucci, M. Coletta, Biochem. Biophys. Res. Commun. 415 (2011) 463–467.
[14] A.A. Kapralov, N. Yanamala, Y.Y. Tyurina, L. Castro, A. Samhan-Arias, Y.A. Vladimirov, A. Maeda, A.A. Weitz, J. Peterson, D. Mylnikov, V. Demicheli, V. Tortora, J. Klein-Seetharaman, R. Radi, V.E. Kagan, Biochim. Biophys. Acta 1808 (2011) 2147–2155.
[15] A. Patriarca, F. Polticelli, M.C. Piro, F. Sinibaldi, G. Mei, M. Bari, R. Santucci, L. Fiorucci, Arch. Biochem. Biophys. 522 (2012) 62–69.
[16] B.S. Rajagopal, G.G. Silkstone, P. Nicholls, M.T. Wilson, J.A. Worrall, Biochim. Biophys. Acta 1817 (2012) 780–791.
[17] G. Silkstone, S.M. Kapetanaki, I. Husu, M.H. Vos, M.T. Wilson, Biochemistry 51 (2012) 6760–6766.
[18] B.S. Rajagopal, A.N. Edzuma, M.A. Hough, K.L. Blundell, V.E. Kagan, A.A. Kapralov, L.A. Fraser, J.N. Butt, G.G. Silkstone, M.T. Wilson, D.A. Svistunenko, J.A. Worrall, Biochem. J. 456 (2013) 441–452.
[19] P. Ascenzi, M. Marino, C. Ciaccio, R. Santucci, M. Coletta, IUBMB Life 66 (2014) 438–447.
[20] P. Ascenzi, M. Marino, F. Polticelli, R. Santucci, M. Coletta, J. Biol. Inorg. Chem. 19 (2014) 1195–1201.
[21] H.M. Marques, Dalton Trans. (2007) 4371–4385.
[22] M.T. Wilson, R.J. Ranson, P. Masiakowski, E. Czarnecka, M. Brunori, Eur. J. Biochem. 77 (1977) 193–199.
[23] S. Pfeiffer, A.C. Gorren, K. Schmidt, E.R. Werner, B. Hansert, D.S. Bohle, B. Mayer, J. Biol. Chem. 272 (1997) 3465–3470.
[24] S. Herold, S. Kalinga, Biochemistry 42 (2003) 14036–14046.
[25] S. Herold, S. Kalinga, T. Matsui, Y. Watanabe, J. Am. Chem. Soc. 126 (2004) 6945–6955.
[26] S. Herold, M. Exner, F. Boccini, Chem. Res. Toxicol. 16 (2003) 390–402.
[27] P. Ascenzi, M. Fasano, Biochem. Biophys. Res. Commun. 353 (2007) 469–474.
[28] P. Ascenzi, P. Visca, Methods Enzymol. 436 (2008) 317–337.
[29] S. Goldstein, G. Merényi, Methods Enzymol. 436 (2008) 49–61.
[30] D.S. Bohle, P.A. Glassbrenner, B. Hansert, Methods Enzymol. 269 (1996) 302–311.
[31] W.H. Koppenol, R. Kissner, J.S. Beckman, Methods Enzymol. 269 (1996) 296–302.
[32] S. Herold, T. Matsui, Y. Watanabe, J. Am. Chem. Soc. 123 (2001) 4085–4086.
[33] S. Goldstein, J. Lind, G. Merényi, Chem. Rev. 105 (2005) 2457–2470.
[34] K.M. Miranda, M.G. Espey, D.A. Wink, Nitric Oxide 5 (2001) 62–71.
[35] P. Ascenzi, A. Bocedi, M. Bolognesi, G. Fabozzi, M. Milani, P. Visca, Biochem. Biophys. Res. Commun. 339 (2006) 450–456.
[36] M.H. Zou, A. Daiber, J.A. Peterson, H. Shoun, V. Ullrich, Arch. Biochem. Biophys. 376 (2000) 149–155.
[37] P. Ascenzi, A. di Masi, M. Coletta, C. Ciaccio, G. Fanali, F.P. Nicoletti, G. Smulevich, M. Fasano, J. Biol. Chem. 284 (2009) 31006–31017.
[38] R. Kissner, W.H. Koppenol, J. Am. Chem. Soc. 124 (2002) 234–239.
[39] M. Mehl, A. Daiber, S. Herold, H. Shoun, V. Ullrich, Nitric Oxide 3 (1999) 142–152.
[40] R. Shimanovich, J.T. Groves, Arch. Biochem. Biophys. 387 (2001) 307–317.
[41] A. di Masi, F. Gullotta, A. Bolli, G. Fanali, M. Fasano, P. Ascenzi, FEBS J. 278 (2011) 654–662.
[42] P. Ascenzi, M. Coletta, Y. Cao, V. Trezza, L. Leboffe, G. Fanali, M. Fasano, A. Pesce, C. Ciaccio, S. Marini, M. Coletta, PLoS One 8 (2013) e69762.
[43] D. Coppola, D. Giordano, M. Tinajero-Trejo, G. di Prisco, P. Ascenzi, R.K. Poole, C. Verde, Biochim. Biophys. Acta 1834 (2013) 1923–1931.
[44] P. Ascenzi, L. Leboffe, A. Pesce, C. Ciaccio, D. Sbardella, M. Bolognesi, M. Coletta, PLoS One 9 (2014) e95391.
[45] F. Sinibaldi, B.D. Howes, E. Droghetti, F. Polticelli, M.C. Piro, D. Di Pierro, L. Fiorucci, M. Coletta, G. Smulevich, R. Santucci, Biochemistry 52 (2013) 4578–4588.
[46] C. Meneghini, L. Leboffe, M. Bionducci, G. Fanali, M. Meli, G. Colombo, M. Fasano, P. Ascenzi, S. Mobilio, PLoS One 9 (2014) e104231.
[47] L. Banci, I. Bertini, H.B. Gray, C. Luchinat, T. Reddig, A. Rosato, P. Turano, Biochemistry 36 (1997) 9867–9877.
[48] A. Pesce, S. Dewilde, M. Nardini, L. Moens, P. Ascenzi, T. Hankeln, T. Burmester, M. Bolognesi, Structure 11 (2003) 1087–1095.
[49] S. Herold, A. Fago, R.E. Weber, S. Dewilde, L. Moens, J. Biol. Chem. 279 (2004) 22841–22847.
[50] M. Momenteau, C.A. Reed, Chem. Rev. 94 (1994) 659–698.
[51] A.B. Sorokin, Chem. Rev. 113 (2013) 8152–8191.
[52] G. Fanali, A. di Masi, V. Trezza, M. Marino, M. Fasano, P. Ascenzi, Mol. Aspects Med. 33 (2012) 209–290.